Current-Dependent Grounding Resistance Model Based on Energy Balance of Soil Ionization

Shozo Sekioka, Maria I. Lorentzou, Maria P. Philippakou, and John M. Prousalidis, *Member, IEEE*

***Abstract*—Soil ionization occurs around a grounding electrode when current density in the soil exceeds a critical value and reduces grounding resistance. This paper proposes a current- dependent grounding resistance model considering the soil ionization. The proposed model is derived on the basis of energy balance of the soil ionization. The resistivity of the ionization zone depends on energy stored in the zone. Analytical expressions of the model are proposed to estimate the zone resistivity. The model is verified by comparing it with experimental results.**

***Index Terms*—Current dependence, energy balance, grounding resistance, hysteresis effect, soil ionization.**

I. Introduction

THE grounding resistance decreases as injected current increases. This phenomenon is caused by soil ionization around a grounding electrode [1]–[11]. Two approaches to calculate the nonlinear grounding resistance considering the soil ionization have been investigated. The first one considers resistivity and dimension of the soil ionization zone. The other one is determined from an empirical relation of the voltage–current curve [12]. Bellaschi introduced effective radius and length, which depend on the injected current of a driven rod to estimate the current dependence of the grounding resistance. The ionized zone with low resistivity grows with the increase of the injected current as illustrated in Fig. 1. Assuming that the zone resistivity is zero, Bellaschi's model is convenient to estimate the current-dependent grounding resistance. However, the zone resistivity does not suddenly become zero. Liew and Darveniza proposed a dynamic grounding resistance model, which considers the zone resistivity and the hysteresis effect [4]. The zone resistivity in their model is a function of time and current density. Calculated results using the Liew–Darveniza model agree satisfactorily with experimental results. However, the physical meaning and derivation of the model are not mentioned sufficiently.

The soil ionization is affected by many factors, such as soil resistivity, temperature, and water content. Considering the soil ionization is similar to the discharge [13], the soil ionization should be represented according to an energy balance, which associates the input energy with the variation of the resistivity. Empirical formulas to represent the current dependence of the grounding resistance as a function of the crest value of the applied current are used to simulate the overvoltages of transmission lines [14]. The formula takes the hysteresis effect into no account, and the simulation results using the formula show low accuracy in the wavetail. Thus, a more accurate model should be developed to consider parameters which affect the grounding resistance. This paper proposes a new current-dependent grounding resistance model based on an energy balance of the soil ionization. The proposed model is determined by the electrode dimension, the injected current, and the energy stored in the ionization zone. Analytical expressions of the model are derived and discussed. One of the authors carried out a number of experiments of the grounding resistance for high-impulse currents [7]–[9]. The proposed model is verified by comparing it with the experimental results.

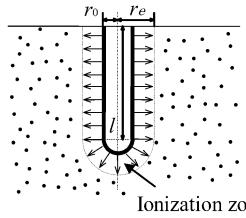

Fig. 1. Illustration of a rod electrode associated with soil ionization.

II. Measured Results of Current-Dependent Grounding Resistance of Rod Electrode

Fig. 2 shows the measured grounding resistance of a reinforced concrete pole (radius $r_0 = 168$ mm, length $l = 2$ m) and a driven rod ($r_0 = 7$ mm, $l = 1.5$ m) for high-impulse currents [9]. The time-to-crest voltage does not coincide with that of applied current due to time dependence and an inherent hysteresis effect of soil ionization. This paper adopts the following definition of the grounding resistance for high-impulse currents [8]

$$R_s(I_m) = \frac{V_m}{I_m} \tag{1}$$

where V_m is the crest electrode voltage (V), I_m is the crest applied current (A), and $R_s(I_m)$ is the grounding resistance for current I_m (Ω).

The low-impulse current generator (LIG) circuit in Fig. 2 is different from the high-impulse current generator (HIG) circuit due to the existence of a damping resistor, which is connected between a grounding electrode for testing and a current lead conductor of the HIG circuit to reduce the applied current. The current waveform of the LIG circuit is different from that of the

Manuscript received February 26, 2004; revised September 27, 2004. Paper no. TPWRD-00087-2004.

S. Sekioka is with Shonan Institute of Technology, Kanagawa 251-8511, Japan.

M. I. Lorentzou is with the Hellenic Transmission System Operator, Athens 17122, Greece.

M. P. Philippakou is with the Public Power Corporation, Athens 10433, Greece.

J. M. Prousalidis is with the National Technical University of Athens, Athens 15773, Greece.

Digital Object Identifier 10.1109/TPWRD.2005.852337

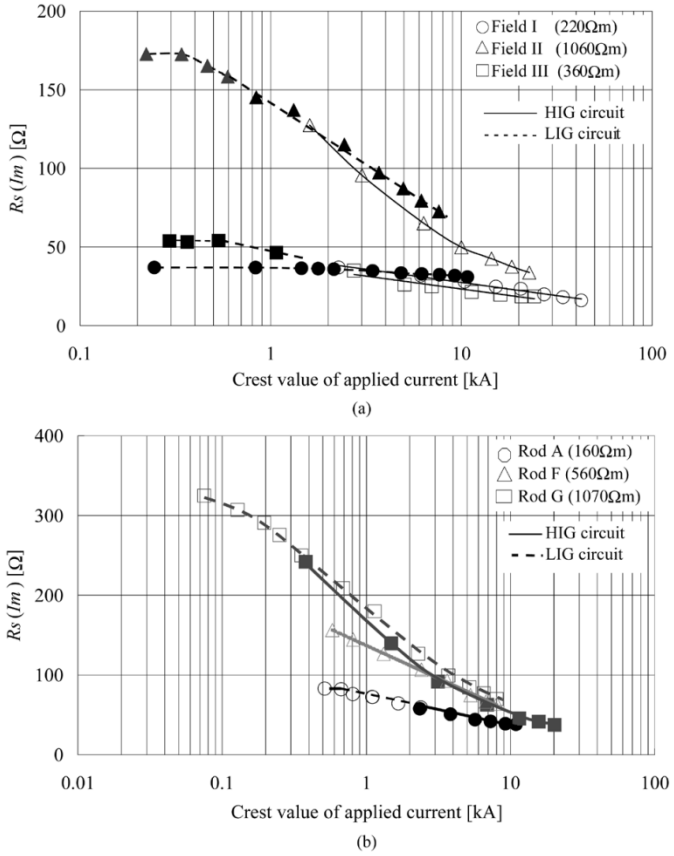

Fig. 2. Measured results of current-dependent grounding resistance as a parameter of soil resistivity. (a) Reinforced concrete pole. (b) Driven rod.

HIG circuit by the damping resistor as shown in Appendix A. The soil resistivity in Fig. 2 is estimated from the measured steady- state grounding resistance without soil ionization shown in Table I using the formula [4]

$$R_s = \frac{\rho_0}{2\pi l} \ln\left(1 + \frac{l}{r_0}\right) \tag{2}$$

where ρ_0 is the soil resistivity with no soil ionization (Ωm).

The actual soil resistivitiy is not uniformly distributed, and the resistivities in Fig. 2(b) differ from those in Fig. 2(a).

It is clear from Fig. 2 that the grounding resistance is greatly dependent on the crest value of the applied current, and becomes almost the same value for high-impulse currents of above 10 kA although the soil resistivity is different.

Fig. 3 shows the measured results for rod A, namely the applied current, rod voltage, and grounding resistance time waveforms. All waveforms are presented for several wavetail shapes of applied current [9]. The grounding resistance time function is defined as the ratio of the instantaneous rod voltage over the applied current at the same time instant. Waveform 1 is generated by the HIG circuit, and waveforms 2 to 4 are controlled by varying the length of a rod–rod gap and the value of a resistor, which are connected in series between the top and the grounding of the impulse generator.

The time constant of the grounding resistance of rod A measured using a pulse generator with step current is about 1 μs as shown in Appendix II. This time constant is sufficiently shorter

TABLE I
MEASURED STEADY-STATE GROUNDING RESISTANCE

(a) Reinforced concrete pole.

Test field	I	II	III
Symbol	○	Δ	□
Resistance	44 Ω	217 Ω	73 Ω

(b) Driven rod.

Electrode	Rod A	Rod F	Rod G
Symbol	○	Δ	□
Resistance	92 Ω	318 Ω	610 Ω

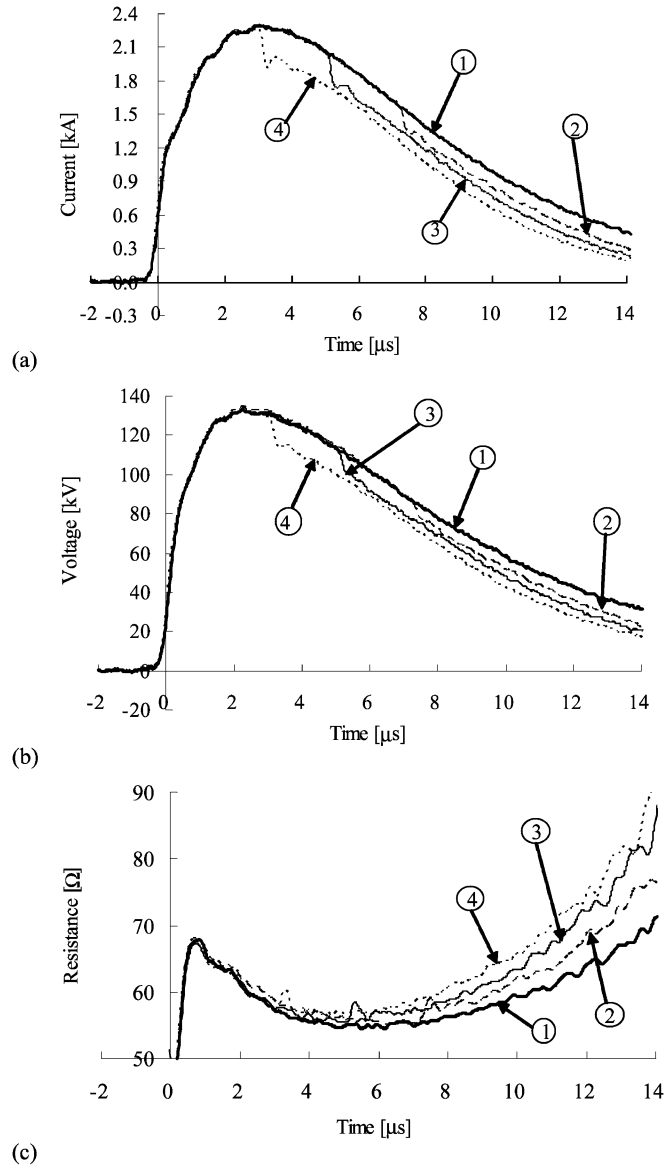

Fig. 3. Measured results for various wavetail shape of the applied current. (a) Applied current. (b) Voltage. (c) Resistance.

than the duration after the applied current is changed in the wavetail, and the transient characteristic of the grounding resistance is negligible for rough estimation. The difference of the grounding resistance is, therefore, affected by the current waveshape, and the zone resistivity depends on the waveshape.

III. Current-Dependent Grounding Resistance Model Based on Energy Balance in Soil Ionization Zone

The nonlinearity of the grounding resistance is represented by the increase of the soil ionization zone and the variation of the zone resistivity. Reference [13] describes a development of the ionization zone by the observation of discharge on X-ray film, which is set under a grounding electrode for testing. The observation results show that the development of the ionization zone shows similar characteristics to that of the discharge in the air. Reference [6] investigates many papers on the soil ionization, and supports the similarity between the soil ionization and the breakdown by air ionization. Energy balance is the foundation stone from which all models describing the discharge process are derived. Thus, the soil ionization can be regarded as a kind of discharge, and the zone resistivity should be determined on the basis of energy balance of the soil ionization.

A. Increase of Soil Ionization Zone

Whenever current density branches off through an electrode and exceeds a critical value, soil ionization occurs. The soil ionization zone of which the resistivity is much lower than the initial soil resistivity grows as the injected current increases. A relation between the critical injected current I_c [A] and the soil ionization gradient E_c (V/m) at a point on the contour of the ionization zone is given by

$$E_c = \rho_0 \frac{I_c}{S(r_c)} \tag{3}$$

where $S(r_c)$ is the surface area of the ionization zone within distance r_c [m] from the grounding electrode.

The contour of the ionization zone for instantaneous injected current i in the wavefront is determined using (3) by substituting i into I_c. The grounding resistance for high currents shows low value in the wavetail [8]. The proposed model assumes that the ionization zone keeps its contour even if the injected current becomes lower than the crest value.

B. Variation of Resistivity of Soil Ionization Zone

The resistivity of the soil ionization zone decreases due to the discharge. The current-dependent grounding resistance can be easily estimated using a simple model, in which the resistivity of the zone is assumed to be zero, by choosing E_c appropriately. However, the resistivity does not suddenly become zero, and depends on such factors as current density, time constant [3], water content [15], and temperature [8]. The grounding resistance gradually recovers its initial value in the wavetail. This fact indicates that the resistivity of the ionization zone increases in the soil deionization process.

C. Energy Balance of Soil Ionization

Energy balance per length of a discharge is given by [16]

$$\frac{dQ}{dt} = ui - P \tag{4}$$

where

- u discharge voltage (V/m);
- i discharge current (A);
- Q accumulated energy (J/m);
- P power loss (W/m);
- t time (s).

The soil ionization process can be considered to be similar to the arc phenomenon occurring inside a circuit breaker during current interruption. Therefore, the accumulated international experience on switch arc modeling can be exploited in the efforts to simulate accurately the soil ionization of grounding systems. Thus, Mayr's equation [17] is the aftermath of processing the energy balance (4)

$$g = K \exp\left(\frac{Q}{Q_0}\right) \tag{5}$$

where g is the arc conductance (Sm), and K (Sm) and Q_0 [J/m] are constants, describing the evolution mechanism of the arc based on the energy balance equation which can be applied, and the following differential equation is derived:

$$\frac{1}{g} \cdot \frac{dg}{dt} = \frac{1}{Q_0}(ui - P). \tag{6}$$

The power loss is generated mainly from heat dissipation/conduction, and should be denoted as a function of temperature and enthalpy. Considering the temperature in the ionization zone might become lower as the distance from the electrode is longer, the heat loss moves outside the ionization zone. This conduction generates the power loss. Thus, the power loss in the proposed model is assumed to be proportional to the surface area of the segment according to Cassie's arc model [18]. The power loss is given by

$$P = \lambda S \tag{7}$$

where λ is constant (W/m^3).

D. Calculation of Grounding Resistance

Equation (6) should be solved with an external electrical circuit simultaneously. An injected current at $t - \Delta t$, where Δt is a time step in calculation, is an approximate solution of exact current by choosing a small Δt in digital simulation. The current i in the proposed model can be regarded as an external force by adopting i at $t - \Delta t$. Thus, the grounding conductance can be estimated as a solution of (6) using the voltage and the current at $t - \Delta t$. The current-dependent grounding resistance $R_s(i)$ is given by summing the resistance of each segment

$$R_s(i) = \int_{r_0}^{r_e} g^{-1}(r)dr + \int_{r_e}^{\infty} g^{-1}(r)dr \tag{8}$$

where r is the distance from the grounding electrode (m), r_e is the effective radius of the ionization zone, and $g(r)$ is the conductance of segment at r.

The proposed model stops calculating the resistivity of a segment when the resistivity reaches the initial value.

A simple model is given by neglecting the first term in (8). Considering the resistivity in the vicinity of the grounding electrode affects the grounding resistance, the simple model needs a high soil ionization gradient so that calculated results using the simple model agree with experimental results [6], [9].

IV. Approximate and General Expressions of Resistivity of Soil Ionization Zone

The differential equation can be solved analytically under an assumption. Analytical expressions of the proposed model are described in this chapter.

A. Approximate Expression of the Proposed Model

After the arc initiation, its electric power input remains approximately constant with the resistivity, rapidly decreasing following the increase of the arc current [19]. This procedure is similar to the one of the soil ionization. Assuming that the electric power input ui or $ui-P$ is independent of the conductance g, the conductance and the resistivity of the soil ionization zone are expressed as follows:

$$g = g_0 \exp\left(\frac{E_n - N}{Q_0}\right) \tag{9}$$

$$\rho = \rho_0 \exp\left(-\frac{E_n - N}{Q_0}\right) \tag{10}$$

where $E_n = \int uidt$ [J/m], $N = \int pdt$ [J/m], and g_0 are the initial conductance of segment, and E_n and N have a unit of energy per length. Therefore, the proposed model shows an energy dependence, and considers an influence of the voltage and current waveform. Fig. 4 illustrates a profile of the resistivity ρ of the soil ionization zone. The resistivity begings to decrease when the injected current exceeds the critical current I_c. The resistivity does not increase rapidly after the injected current begins to decrease, because the energy $E_n - N$ stored in the segment continues to increase for some time. The resistivity gradually increases in the soil deionization process for $ui < P$. As a result, the grounding resistance shows the hysteresis characteristic. This characteristic is observed in experimental results [8].

Equations (8) and (10) indicate that the proposed model has the following physical meanings.

1) *Current dependence*: The higher the injected current is, the soil ionization zone becomes larger. The growth of the zone is equivalent to the increase of the effective radius and reduces the grounding resistance.
2) *Energy dependence*: The zone resistivity decreases as the energy $E_n - N$ stored in the zone increases.
3) *Soil deionization*: When the power input *ui* is less than the power loss P, the zone resistivity increases and, finally, the reduced resistivity recovers the initial value ρ_0.
4) *Hysteresis effect*: The zone resistivity continues to decrease for some time after the injected current takes a crest value, and gradually increases in the soil deionization process. The profile of the zone resistivity in the ionization process is different from that in the deionization process. Thus, the resistivity shows the hysteresis characteristic.

B. General Expression of the Proposed Model

Considering a relation $i = gu$, (6) can be solved, and the conductance and the resistivity are given by

$$g = g_0 \exp\left(\frac{-t}{\tau}\right)\left[1 + \frac{1}{g_0 Q_0}\int i^2 \exp\left(\frac{t}{\tau}\right)dt\right] \tag{11}$$

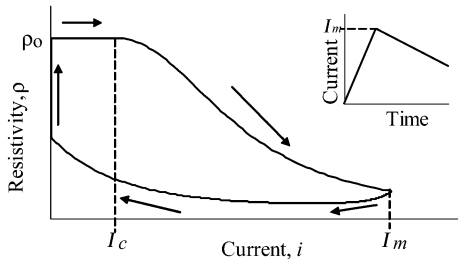

Fig. 4. Profile of resistivity of soil ionization zone.

$$\rho = \rho_0 \exp\left(\frac{t}{\tau}\right)\left[1 + \frac{1}{g_0 Q_0}\int i^2 \exp\left(\frac{t}{\tau}\right)dt\right]^{-1} \tag{12}$$

where t is the instantaneous time after the soil ionization in a segment occurs (s) $\tau = Q_0/P$ [s].

Substituting $i = 0$ into (12) when ρ becomes ρ_i

$$\rho = \rho_i \exp\left(\frac{t'}{\tau}\right) \tag{13}$$

where $t' = 0$ at which the current just becomes zero, is obtained. Equation(13) indicates that τ means the time constant of the resistivity in recovering the initial value.

Equations (11) and (12) include a divergence function $\exp(t/\tau)$, and the calculation of the general expression often results in numerical divergence. Appendix III describes a method to calculate (11) and (12).

V. Discussion

A. Comparison of the Proposed Model With the Liew–Darveniza Model

Setting $(ui - P)/Q_0 = \alpha$ (constant), (10) is written as follows:

$$\rho = \rho_0 \exp(-\alpha t). \tag{14}$$

Equation (14) is the same as the Liew–Darveniza model in the soil ionization process. On the other hand, the Liew–Darveniza model in the deionization process, is given by

$$\rho = \rho_i + (\rho_0 - \rho_i)\left(1 - \exp\frac{-t}{\tau_2}\right)\left(1 - \frac{J}{J_C}\right)^2 \tag{15}$$

where

τ_2 deionization time constant (s);
J current density $(\mathrm{A/m^2})$;
J_c critical current density;
ρ_i resistivity at $J = J_c$ on current decay is different from that in the ionization process.

When $J = 0$, (15) yields

$$\rho = \rho_i + (\rho_0 - \rho_i)\left(1 - \exp\frac{-t}{\tau_2}\right). \tag{16}$$

Equation (16) is different from (13). Time constant τ_d is defined by

$$\tau_d = \int_0^T \left(1 - \frac{\rho}{\rho_0}\right)dt \tag{17}$$

where T is the time when ρ reaches ρ_0 is introduced to compare the transient characteristics of the resistivity. The time constant of the soil deionization is obtained by substituting (13) and $T = \tau \ln(\rho_0/\rho_i)$ of the proposed model, and (16) and $T = \infty$ of the Liew–Darveniza model into (17) as follows as shown in (18) at the bottom of the page, where $k = \rho_i/\rho_0$.

Considering k is sufficiently less than unity, the deionization time constant of the Liew–Darveniza model is a few times longer than that of the proposed model if τ_d takes the same value. Accordingly, the variation of the resistivity from the lowest value to the initial one of the Liew–Darveniza model using a larger deionization time constant is almost same as that of the proposed model. Thus, the Liew–Darveniza model is one kind of the proposed model, while the proposed model provides a physical meaning of their model.

B. Constants of the Proposed Model

1) *Soil ionization gradient* E_c: E_c of 300 kV/m [6], 400 kV/m [14], and 1000 kV/m [5] are recommended. Thus, the value is not established. A low value should be selected to consider the resistivity of the soil ionization zone.
2) *Power loss* λ: When the soil ionization just starts, namely $i = I_c$, ρ is equal to ρ_0. Accordingly, the following relation should be satisfied from (10):

$$(ui - P)_{i=Ic} = 0. \tag{19}$$

From (3), (7), and (19), the following relation is obtained:

$$uI_c - P = S\left(\frac{E_c^2}{\rho_0} - \lambda\right) = 0$$
$$\therefore \lambda = \frac{E_c^2}{\rho_0}. \tag{20}$$

The soil ionization can be regarded to occur when input power becomes greater than a critical value.
3) Q_0: Fig. 5 shows the calculated results of the evolution in time of the grounding resistance used in the measurements for parameters of Q_0 and ρ_0 by the general expression, where the applied current has ramp waveform of 2/40 μs and $E_c = 300$ kV/m.

The time constant of the soil ionization is proportional to Q_0. Consequently, the grounding resistance decreases faster as Q_0 is smaller and, finally, becomes almost the same value as shown in Fig. 5(a). Fig. 5(b) indicates that the current dependence of the grounding resistance is greater as Q_0 is smaller, but the influence of Q_0 becomes smaller as the applied current is higher.

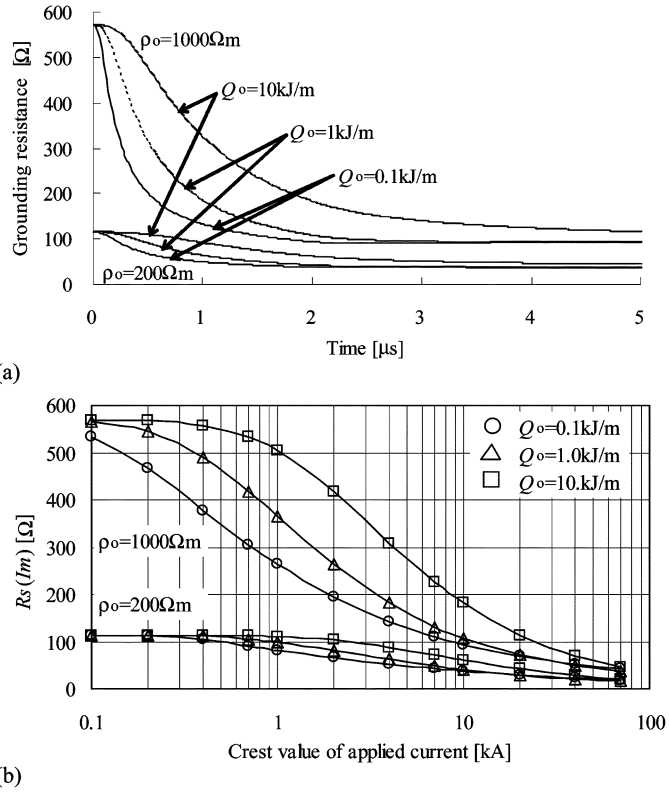

Fig. 5. Influence of Q_0 on the current dependence of grounding resistance. (a) Influence of Q_0 on variation of grounding resistance for applied current of 10 kA. (b) Influence of Q_0 on current dependence of grounding resistance.

C. Validation of the Proposed Model in Comparison of Calculated Results With Experimental Results

Figs. 6 and 7 show the calculated results of the grounding resistance corresponding to Figs. 2(b) and 3(c) by using the general expression. The constants of the proposed model are shown in Table II and $\Delta r = 2$ mm, where Δr is the width of the segment. Time dependence of the grounding resistance is represented by an equivalent circuit in Fig. 12(b). The current dependence of each resistance of the circuit is assumed to be proportional to that of the total grounding resistance, while the capacitances of the equivalent circuit are not dependent on the current. Calculated results by the Liew–Darveniza model are included in Fig. 6.

It is clear from the comparison of the calculated results with the measured ones that the proposed model shows sufficient accuracy. The difference between the measured and calculated results is caused possibly by the simplifying assumption of the energy loss expressed in (7), and the time dependence of the equivalent circuit. The Liew–Draveniza model shows sufficient accuracy for low currents, as the error of the their model increases as the applied current increases too.

$$\tau_d = \begin{cases} \tau\left[-\ln k - (1-k)\right] \approx \tau \sum_{n=2}^{\infty} \frac{(1-k)^n}{n}; & \text{proposed model} \\ \tau_2(1-k); & \text{Liew–Darveniza model} \end{cases} \tag{18}$$

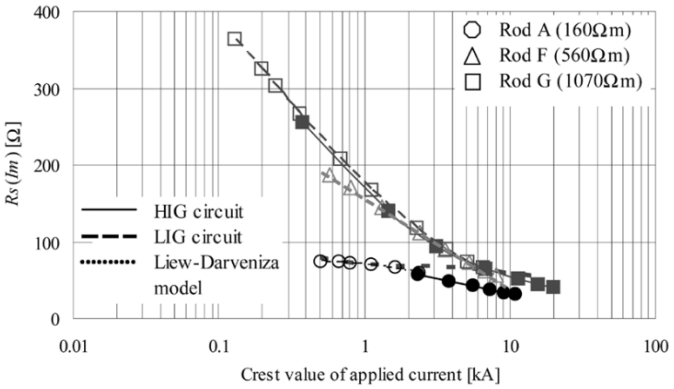

Fig. 6. Calculated results of current dependence of grounding resistance of the driven rod.

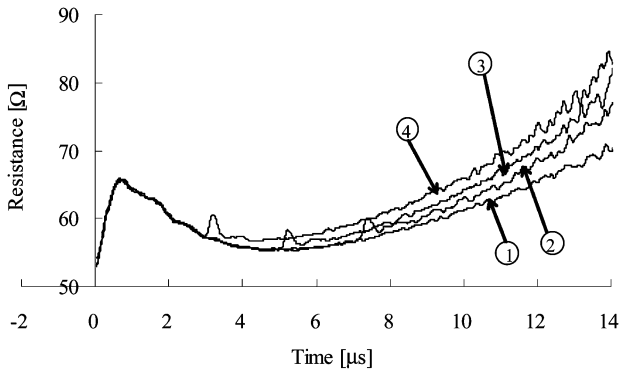

Fig. 7. Calculated results of grounding resistance for the various wavetail shape of applied current.

TABLE II
Q_0 AND λ

ρ_0 [Ωm]	160	560	1070
Ec [kV/m]	330	110	110
λ [MW/m^3]	680	21.6	11.3
Q_0 [J/m]	1800	600	150

D. Comparison of the Approximate Expression with the General Expression

This section investigates the accuracy of the approximate expression by comparing it with the general one. Fig. 8 shows the error of the approximate expression in comparison with the general one in cases corresponding to Fig. 5.

Fig. 8 shows that the error of the approximate expression is proportional to $I_m^{3/4}$. The approximate expression shows sufficient accuracy for less than 10 kA.

VI. CONCLUSION

This paper has proposed a current-dependent grounding resistance model based on an energy balance of soil ionization. The proposed model considers the increase of the soil ionization zone and the variation of the zone resistivity to represent the current dependence. The model is denoted by a function of energy stored in the ionization zone, and shows a hysteresis effect of the grounding resistance. Approximate and general expressions of the proposed model have been described. The model gives physical meanings of the nonlinear characteristics such as the current dependence and the hysteresis effect of the grounding resistance due to the soil ionization and deionization. The model has been verified by comparing it with experimental results.

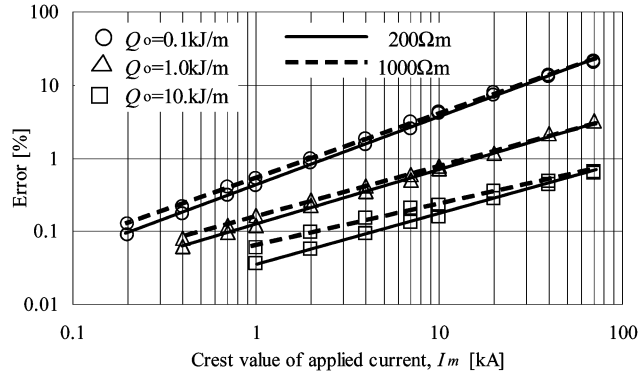

Fig. 8. Error of the approximate expression in comparison to the general one.

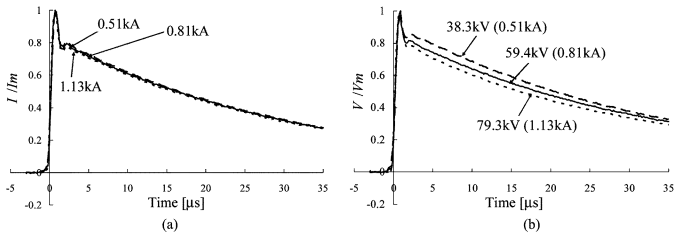

Fig. 9. Measured results of voltages and applied currents of rod A by the LIG circuit. (a) Current. (b) Voltage.

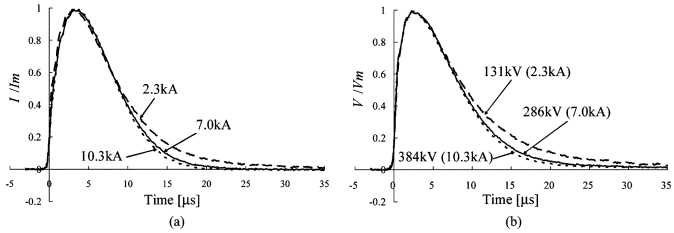

Fig. 10. Measured results of voltages and applied currents of rod A by the HIG circuit. (a) Current. (b) Voltage.

APPENDIX A

Current and Voltage Waveforms

Figs. 9 and 10 show the measured waveforms of applied currents and voltages, which are normalized by the crest value. Hysteresis characteristics of the grounding resistance are shown in Fig. 11. The grounding resistance for low currents during the wavefront is increased. This phenomenon is caused by the time dependence having capacitive variation. The current dependence can be clearly observed after a while.

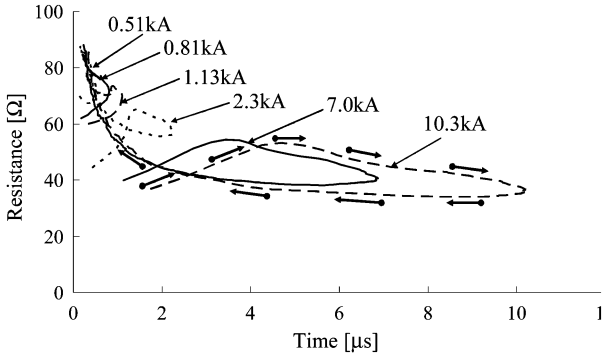

Fig. 11. Measured results of hysteresis characteristics.

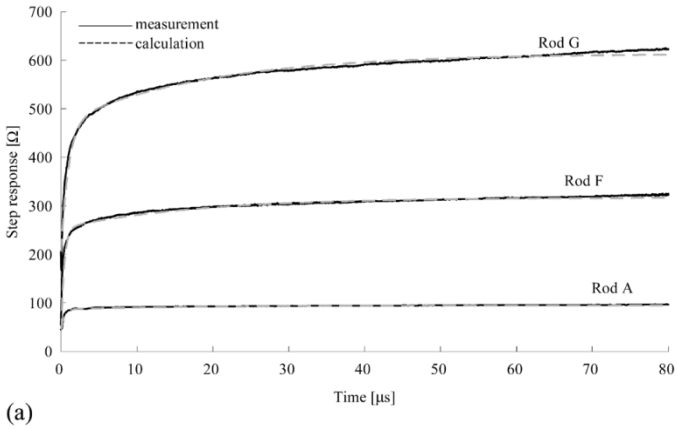

(a)

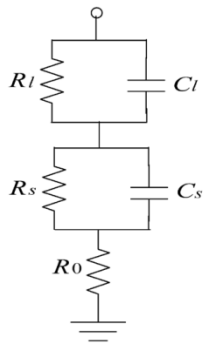

(b)

Fig. 12. Grounding resistance for a low current. (a) Step response (b) Equivalent circuit.

TABLE III
CONSTANTS OF THE EQUIVALENT CIRCUIT OF RODS A, F, AND G

	R_l [Ω]	C_l [μF]	R_s [Ω]	C_s [nF]	R_0 [Ω]
Rod A	8.0	2.3	42.0	11.0	45.0
Rod F	63.0	0.28	213	2.0	41.0
Rod G	143	0.14	266	3.7	205

APPENDIX B

Transient Characteristic of Rods A, F, and G

Fig. 12 shows the step response of the grounding resistance and an equivalent circuit of the rod electodes A, F, and G. The step response is obtained from the measured voltage and current with no soil ionization by using a numerical Laplace transform (Table III) [20].

APPENDIX C

A Method to Calculate (11) and (12)

The following variable is introduced:

$$Y(t) = e^{-(t/\tau)} \int_0^t i^2(T) e^{(T/\tau)} dT \tag{21}$$

where $\exp(t)$ for a large value diverges in digital simulation, and it is impossible to directly calculate (11) and (12). $Y(t)$ is written by

$$\begin{aligned} Y(t) &= e^{-(\Delta t/\tau)} \\ &\quad \times \left[Y(t-\Delta t) + e^{-(t-\Delta t/\tau)} \int_{t-\Delta t}^{t} i^2(T) e^{(T/\tau)} dT \right] \\ &\approx e^{-(\Delta t/\tau)} \\ &\quad \times \left[Y(t-\Delta t) + e^{-(t-\Delta t/\tau)} i^2(t-\Delta t) e^{(t-\Delta t/\tau)} \Delta t \right] \\ &= \exp\left(\frac{-\Delta t}{\tau}\right) \left[Y(t-\Delta t) + i^2(t-\Delta t)\Delta t \right]. \end{aligned} \tag{22}$$

where $Y(t)$ is calculated using a past value of $Y(t)$, the injected current, and $\exp(\Delta t/\tau)$. Therefore, (22) gives a numerical stability in calculating (11) and (12) by choosing a small Δt.

REFERENCES

[1] P. L. Bellaschi, "Impulse 60-cycle characteristics of driven grounds," *AIEE Trans.*, vol. 60, pp. 123–128, 1941.
[2] P. L. Bellaschi, R. E. Armington, and A. E. Snowdon, "Impulse 60-cycle characteristics of driven grounds," *AIEE Trans.*, pt. II, vol. 61, pp. 349–363, 1942.
[3] A. V. Korsuntcev, "Application of the theory of similitude to the calculation of concentrated earth electrodes," *Electrichestvo*, no. 5, pp. 31–35, 1958.
[4] A. C. Liew and M. Darveniza, "Dynamic model of impulse characteristics of concentrated earth," *Proc. Inst. Elect. Eng.*, vol. 121, pp. 123–135, 1974.
[5] E. E. Oettle, "A new general estimation curve for predicting the impulse impedance of concentrated earth electrodes," *IEEE Trans. Power Del.*, vol. 3, no. 4, pp. 2020–2029, Oct. 1988.
[6] A. M. Mousa, "The soil ionization gradient associated with discharge of high currents into concentrated electrodes," *IEEE Trans. Power Del.*, vol. 9, no. 3, pp. 1669–1677, Jul. 1994.
[7] T. Matsui, M. Adachi, H. Fukuzono, S. Sekioka, O. Yamamoto, and T. Hara, "Measurements of grounding resistances of a transmission-line tower base connected with auxiliary grounding electrodes for high impulse currents," in *Proc. 10th Int. Symp. High Voltage Engineering*, vol. 5, Montreal, QC, Canada, 1997, pp. 257–260.
[8] S. Sekioka, H. Hayashida, T. Hara, and A. Ametani, "Measurements of grounding resistances for high impulse currents," *Proc. Inst. Elect. Eng., Gen., Transm. Distrib.*, vol. 145, no. 6, pp. 693–699, 1998.
[9] S. Sekioka, T. Sonoda, and A. Ametani, "Experimental study of current-dependent grounding resistances of rod electrode," *IEEE Trans. Power Del.*, vol. 20, no. 2, pp. 1569–1576, Apr. 2005.
[10] J. M. Prousalidis, M. P. Philippakou, N. D. Hatziargyriou, and B. C. Papadias, "The effect of ionization in wind turbine grounding modeling," in *Proc. Mediterranean Electrotechnical Conf.*, Cyprus, 2000, pp. 28–31.
[11] M. I. Lorentzou, N. D. Hatziargyriou, and B. C. Papadias, "Time domain analysis of grounding electrodes impulse response," *IEEE Trans. Power Del.*, vol. 18, no. 2, pp. 517–5124, Apr. 2003.
[12] "Perspectives on soil ionization," in *Proc. International Conference on Grounding and Earthing*, Belo Horizonte, Brazil, 2000, CIGRE Task Force on Soil Ionization—WG 33.01, pp. 105–106.

[13] M. Hayashi, "Observation of streamer in the soil by surge current" (in Japanese), *J. Inst. Elect. Eng. Jpn.*, vol. 87-1, pp. 133–141, 1967.
[14] "Guide to Procedures for Estimating the Lightning Performance of Transmission Lines,", CIGRE Working Group 33.01, 1991.
[15] D. P. Snowdon and J. W. Erler, "Initiation of electrical breakdown of soil by water vaporization," *IEEE Trans. Nucl. Sci.*, vol. 30, no. 6, pp. 4568–4571, Dec. 1983.
[16] "Applications of Black Box Modeling to Circuit Breakers," *ELECTRA*, no. 139, pp. 40–71, 1993.
[17] O. Mayr, "Beitrage zur theorie des statschen und des dynamischen lichtbogens," *Arch. fur Elektrotechnik*, vol. 37, pp. 588–608, 1943.
[18] A. M. Cassie, "Arc Rupture and Circuit Severity: A New Theory," CIGRE, Paris, France, Report no. 102, 1939.
[19] T. Inaba, "Analytical similarity between stabilized arc characteristics and transport properties in gases" (in Japanese), *Trans. Inst. Elect. Eng. Jpn.*, vol. 94-A, no. 3, pp. 83–90, 1974.
[20] A. Ametani, "The application of the fast Fourier transform to electrical transients phenomena," *Int. J. Elect. Eng. Educ.*, vol. 10, pp. 277–281, 1973.

Shozo Sekioka was born in Osaka, Japan, on December 30, 1963. He received the B.Sc. and D.Eng. degrees from Doshisha University, Kyoto, Japan, in 1986 and 1997, respectively.

He was with Kansai Tech Corporation, Osaka, Japan, from 1987 to 2005, and then he joined the Department of Electrical and Electronic Media Engineering, Shonan Institute of Technology, Kanagawa, Japan. He has been engaged in lightning surge analysis in electric power systems.

Maria I. Lorentzou was born in 1971. She received the Ph.D. degree from the electrical and computer engineering department, National Technical University of Athens (NTUA), Athens, Greece, in 2001.

Currently, she is with the Hellenic Transmission System Operator (HTSO). Her research interests include the transient behavior of grounding systems, lightning protection of wind turbines, and calculation of power system transients.

Dr. Lorentzou is a member of the Technical Chamber of Greece.

Maria P. Philippakou was born in Athens, Greece, on October 18, 1969. She received the Diploma and Ph.D. degrees in electrical and computer engineering from the National Technical University of Athens, Athens, Greece, in 1992 and 1999, respectively.

In 2000, she joined the Public Power Corporation (PPC), Thermal Projects, and has been engaged in the thermal Power Plant Electrical Engineering and Construction Dept.

John M. Prousalidis (M'93) was born in Athens, Greece, on December 16, 1968. He received the Diploma and Ph.D. degrees in electrical and computer engineering from the National Technical University of Athens (NTUA), in 1991 and 1997, respectively.

In 2001, he was a Lecturer with the Academic Staff of the Naval Architecture and Marine Engineering Department of NTUA, dealing with marine electrical engineering issues.